Infrared, Raman, and Inelastic Neutron Scattering Spectra of Dodecahedrane: an I_h Molecule in T_h Site Symmetry

Bruce S. Hudson,*,† Damian G. Allis,† Stewart F. Parker,‡ Anibal J. Ramirez-Cuesta,‡ Henryk Herman,§ and Horst Prinzbach||

Department of Chemistry, Syracuse University, Syracuse, New York 13244-4100, ISIS Facility, Rutherford Appleton Laboratory, Chilton, Didcot OX11 0QX, U.K., Department of Chemistry, University of Surrey, Guildford, Surrey, GU2 5XH, U.K., and Chemisches Laboratorium der Universität, Institute für Organische Chemie und Biochemie, 79104 Freiburg, Germany

Received: January 18, 2005; In Final Form: February 14, 2005

The Raman spectrum of crystalline dodecahedrane, $C_{20}H_{20}$, a species of nominal I_h symmetry, exhibits splitting of the H_g Raman active modes. The Raman inactive gerade vibrations of G_g, T_{1g}, and T_{2g} symmetry are found to have weak Raman activity. The IR forbidden vibrations of T_{2u}, G_u, and H_u type have moderate IR activity. All of this is consistent with the T_h site symmetry. A treatment of the structure and vibrations of dodecahedrane using a periodic lattice DFT method results in a slightly distorted T_h structure with six C−C bonds that are 0.001 Å longer than the other 24. The vibrational spectrum computed for this structure exhibits splittings of the H_g modes that are consistent with the observed spectra, but the computed splittings are larger than observed in room-temperature data. A complex pattern observed in the C−H stretching region is assigned. The inelastic neutron scattering spectrum calculated from the computed normal modes for the T_h molecule in the lattice agrees quantitatively with experiment when overtone and combination transitions are included and allowance is made for anharmonicity of the C−H stretch motion. Finally, it is argued that the existing crystallographic determination of the average C−C bond length of 1.544 Å is shortened by disorder and should be revised upward to agree with the computed value of 1.558 Å.

Introduction

Dodecahedrane, $C_{20}H_{20}$, is a rare example of an icosahedral symmetry hydrocarbon.[1−6] The vibrational analysis of this species provides a classic case of the application of group theory and vibrational selection rules. The crystal and molecular structure of dodecahedrane are shown in Figure 1. The icosahedral symmetry molecule packs in the cubic $Fm\bar{3}$ (No. 202) space group with T_h site symmetry. This face centered cubic structure has four molecules per unit cell.[7] Under the I_h point group appropriate to the molecule, the 114 normal modes of vibration are classified into $2A_g + 1T_{1g} + 2T_{2g} + 4G_g + 6H_g + 3T_{1u} + 4T_{2u} + 4G_u + 4H_u$ symmetry types. There are only 30 discrete vibrational frequencies due to the high average degeneracy. The three T_{1u} modes are active in the IR spectrum, and the two A_g and six H_g modes are active in the Raman spectrum. The other 19 modes of vibration are forbidden by these optical methods in I_h symmetry. In the T_h site symmetry only 3-fold degeneracy is sustained. The retention of the center of inversion preserves the gerade/ungerade subdivision. The major result of this symmetry lowering, so far as the optical spectra are concerned, is splitting of the Raman active H modes into T and E types and induction of Raman activity in all gerade modes and IR activity in all ungerade modes.

Figure 2 is a survey of the IR, Raman, and inelastic neutron scattering (INS) spectra of dodecahedrane as a polycrystalline solid. The high-frequency C−H stretch region is excluded and will be discussed later. The interpretation of this spectrum in terms of I_h molecular symmetry is straightforward. The IR spectrum reveals the T_{1u} modes at 728 and 1298 cm^{-1} as the strongest features, but there are clearly other features present. The Raman spectrum contains the A_g mode as the strongest feature at 677 cm^{-1} as well as the five H_g modes expected in this region. On the scale of this spectrum these modes appear to be single spectral peaks but are, in fact, split as discussed below. The INS spectrum contains all vibrational features with intensities proportional to the extent of H atom motion. A previous publication[8] compared the intensity distribution of this

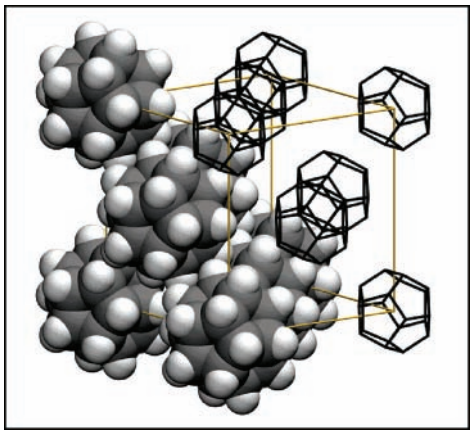

Figure 1. Structure of dodecahedrane in both space-filling and skeletal depictions. The cubic unit cell is comprised of 1/8 of each molecule at the eight corners and 1/2 of each molecule at the six faces for a total of 4. The primitive unit cell has $Z = 1$.

* Corresponding author. E-mail: bshudson@syr.edu.
† Syracuse University.
‡ Rutherford Appleton Laboratory.
§ Univesity of Surrey.
|| Institute fur Organische Chemie und Biochemie.

10.1021/jp0503213 CCC: $30.25
Published on Web 03/26/2005

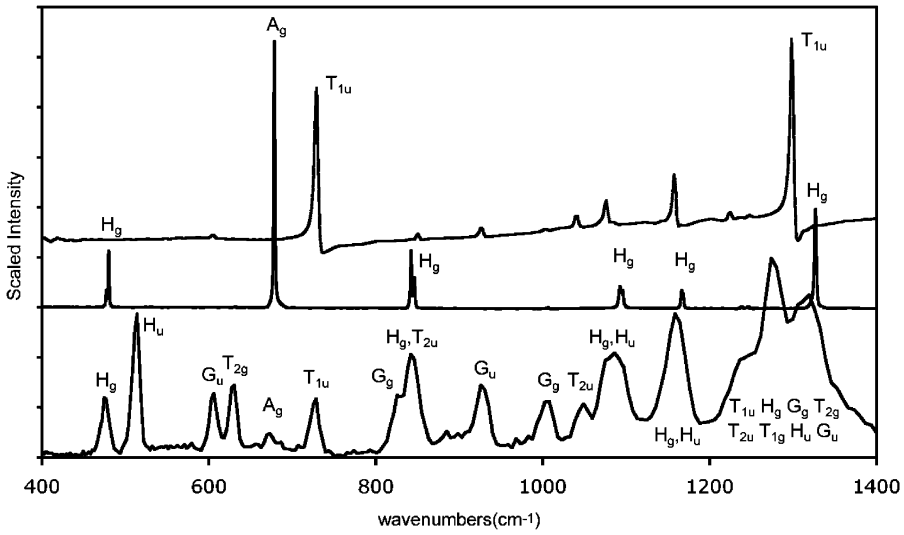

Figure 2. Survey spectra of dodecahedrane showing the IR spectrum (top), Raman spectrum (middle), and INS spectrum (bottom). The symmetry labels refer to I_h symmtery.

TABLE 1: Vibrational Frequencies (in cm^{-1}) for Dodecahedrane[a]

I_h	isolated I_h symmetry B3LYP/6-31G**	crystal cell T_h symmetry PW91/dn (DMol^3)	Raman (this work)	IR (this work)	INS (ref 8)
H_g	481	481.3, 476.5	477.1, 480		477
H_u	518	517.6, 519.4			514
G_u	615	609, 630.5		[605.6]	607
T_{2g}	639	637.2	[632.4]		632
A_g	673	675.4	678.6		675
T_{1u}	731	726.9		729.1	727
G_g	843	835.9, 838.5			(845)
H_g	852	850.5, 842.7	842.6, 846.4		(845)
T_{2u}	866	858.3		[850.6]	(845)
G_u	941	931.5, 943.1		[926]	930
G_g	1016	1017.5, 1007.3	[1006.5]		1007
T_{2u}	1058	1055.8		[1040.6]	1050
H_u	1093	1095.5, 1099.4		[1076.3]	(1089)
H_g	1110	1116.1, 1108.4	1092.7, 1095.7		(1089)
H_u	1192	1148.5, 1151.7		[1157.4]	(1164)
H_g	1198	1171.9, 1160.8	1166.7, 1168.3		(1164)
T_{2u}	1269	1226.4		[1224.8]	1270 sh
G_g	1282	1244, 1240.5	[1246, 1238.5]		1282
T_{1g}	1305	1268.3	[1268.5]		
T_{2g}	1309	1274.7	[1275]		1310
H_u	1316	1289.3, 1295.4		[1247.9]	1320
T_{1u}	1341	1309.8		1298.1	
G_u	1354	1310.5, 1339.9			1380 sh
H_g	1367	1323.3, 1333.7	1326.9		

[a] Calculated frequencies for the isolated molecule and crystal cell are compared with the Raman and IR frequencies of this work. The Raman and IR frequencies reported in square brackets are induced by the lower symmetry of the crystal field. The isolated molecule calculated values (B3LYP/6-31G**) and INS frequencies are taken from ref 8. The INS values in parentheses are overlapped by other transitions. The isolated molecule calculations result in I_h symmetry with the irreducible representation indicated in the first column. The crystal cell (DMol^3) periodic DFT calculations are performed with T_h site symmetry. This results in splitting of the G and H representations as indicated. This splitting is analyzed in more detail in Table 2. The higher frequency (C−H stretch) vibrations are shown in Table 3. Induced Raman activity is denoted by [ ].

spectrum in the 400−1600 cm^{-1} region with the expectations of a density functional theory (DFT) calculation for the isolated $C_{20}H_{20}$ molecule. The results of this calculation, the frequencies of the INS features, and the IR and Raman spectra are given in Table 1. In the present work we investigate the effects of intermolecular interactions in the crystal on both the optical and INS spectra of dodecahedrane and present the results of a more detailed interpretation of the INS spectrum based on a periodic DFT calculation and with inclusion of overtone and combination transitions. This provides a detailed test of the periodic DFT method and shows that the effect of crystal deformations can be reasonably simulated.

Experimental and Computational Methods

The dodecahedrane was the same high-purity sample as used previously[8] and was synthesized as described in detail elsewhere.[1,2] The IR spectrum was recorded as a KBr disk using a Digilab FTS-60 with a DTGS detector using 128 scans at 4 cm^{-1} resolution. The absolute precision of the spectrum was determined by calibration using a National Physical Laboratory (Teddington, UK) certified polystyrene film. The Raman spectrum was obtained with a Perkin-Elmer System 2000 FT Raman spectrometer with 1064 nm excitation and a room-temperature InGaAs detector. Fifty-five scans were collected at 0.5 cm^{-1} resolution with 400 mW incident laser power from

the pure solid held in a quartz cuvette. The INS experiments were carried out using the TOSCA instrument[9−11] at the ISIS facility of the Rutherford Appleton Laboratory as previously described.[8]

Isolated molecule and solid-state density functional theory (DFT) calculations were performed with the program[12−15] DMol^3 on the SGI Origin Array at the National Center for Supercomputing Applications (NCSA). Both the $Fm\bar{3}$ unit cell ($Z = 4$), reported in ref 1 and available from the Inorganic Crystal Structure Database, and its primitive cell ($Z = 1$) were analyzed. The dn numerical basis set and PW91 generalized gradient approximation density functional[16] were employed for all calculations (PW91/dn). The PW91 density functional was chosen from among those available in DMol^3 for its adequate reproduction of the isolated molecule geometry and normal-mode frequencies prior to the computationally demanding solid-state calculations. The dn basis set is reported to compare favorably with the 6-31G basis set. PW91/dn vibrational modes were left unscaled. Due to the large size of the $Fm\bar{3}$ ($Z = 4$, $a = b = c = 10.644$ Å, $\alpha = \beta = \gamma = 90°$) unit cell, the grid spacing was set to the program option "medium" (corresponding to a k-point separation of 0.05 Å^{-1}) and the energy convergence to 5.0×10^{-6} hartree for the geometry optimization and normal-mode analysis. The primitive cell ($Z = 1$, $a = b = c = 7.527$ Å, $\alpha = \beta = \gamma = 60°$) was examined with both the "medium" criteria above (for comparison with the $Z = 4$ calculations) and "fine" criteria (corresponding to a k-point spacing of 0.04 Å^{-1} and an energy convergence of 1×10^{-6} hartree). In both cases, the degenerate mode components in the molecular T_h point group were degenerate to within 0.1 cm^{-1}. The isolated molecule PW91/dn geometry optimization and normal-mode analysis was performed with the "fine" criteria specified above. These same criteria were used for a single-point energy and normal-mode analysis of an isolated T_h-symmetry dodecahedrane (from the "fine" primitive cell). This T_h-symmetry dodecahedrane calculation was performed to determine the degree of the H and G (I_h) mode splittings in the absence of the crystal environment, or the degree of splittings due only to molecular (T_h) deformation. Efforts to reproduce the normal-mode degeneracy of the H and G modes in the I_h isolated molecule calculations were unsuccessful with the "medium" settings. Because the isolated molecule was of I_h symmetry both in bond lengths and in overall structure in the less stringent geometry optimization, the problem with degeneracy reproduction in the isolated case is presumed to be a limit of the grid size used during the atomic displacements in the DMol^3 numerical second-derivative calculation. This problem is analogous to the requirement of high-quality DFT grids to adequately treat tetrahedral centers in programs such as Gaussian and GAMESS. Interestingly, this grouping problem did not occur in the periodic calculations. The groupings of the degenerate normal-mode frequencies with tight convergence criteria are adequate for the analysis and assignment of the isolated molecule. The lower symmetry groupings and splittings of these modes in the solid state require greater attention in their analysis because certain degenerate (H and G) modes split into the same narrow vibrational regions. The lack of symmetry assignments in DMol^3 was reconciled with a simple gerade/ungerade analysis performed by summation over the eigenvectors in each normal mode of inversion center related atoms.

Experimental Results

Splitting of the H_g Modes. The 5-fold degenerate Raman active H_g modes split into a T_g and E_g pair. Figure 3 shows expanded sections of the Raman spectrum in the regions of the four lowest energy H_g modes. These modes are all clearly split by as much as 4 cm^{-1}. The intensity distribution suggests that the T mode is higher in energy than the E mode in the lowest frequency pair near 480 cm^{-1} but that the energy of the E mode is higher than that of the T mode in the other three cases shown. The frequencies are given in Table 2. These splittings are discussed below. These data provide our best test of the validity

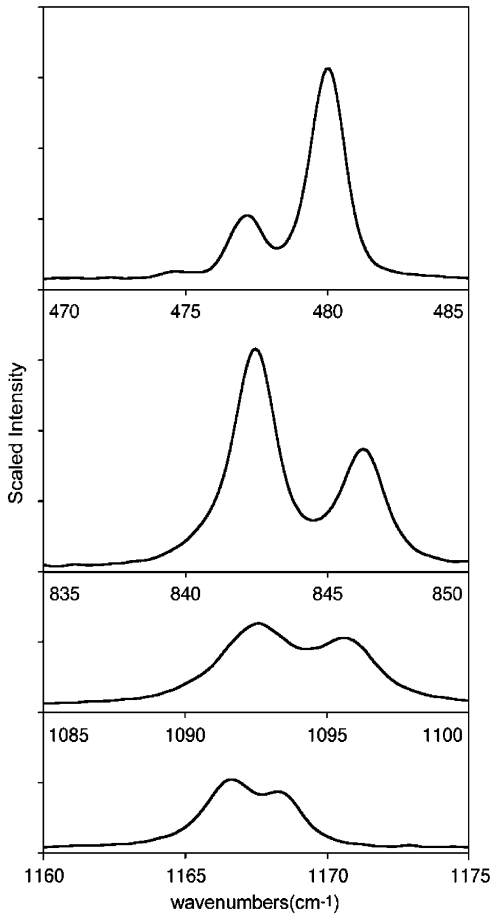

Figure 3. Expanded view of the Raman spectrum of dodecahedrane showing the four low-frequency modes of H_g symmetry in I_h split due to the T_h site symmetry of the primitive $Z = 1$ unit cell. The full horizontal scale is 15 cm^{-1} in each case.

TABLE 2: Calculated and Observed Components of the Raman Active Modes of Dodecahdedrane[a]

calcd		obsd
476.5	E	477.1
481.3	T	480.0
4.8	Δ	2.9
675.4	A	678.5
842.7	E	842.5
850.5	T	846.4
7.8	Δ	3.9
1095.5	T	1092.7
1099.4	E	1095.7
3.9	Δ	3.0
1160.8	E	1166.7
1171.9	T	1168.3
11.1	Δ	1.6
1323.2	E	1326.9
1333.7	T	1326.9
10.5	Δ	0

[a] All modes are of gerade symmetry, and all values are in cm^{-1}.

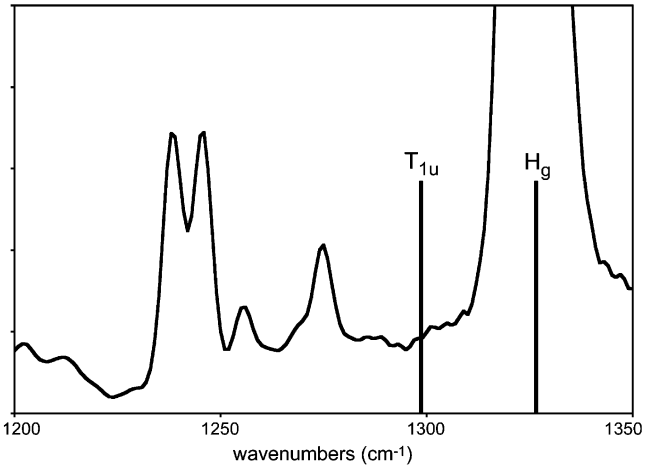

Figure 4. Raman spectrum of dodecahedrane on a vertically expanded scale showing the induced intensity of the I_h symmetry G_g mode due to the lower T_h site symmetry as well as several overtone transitions. The lack of intensity in the T_{1u} symmetry mode is also shown.

of the harmonic approximation used in the calculations. When the calculated and observed splitting components are averaged and compared, the average percent deviation for the six values is 0.05%. The average absolute percent deviation is 0.24%. This difference reflects the fact that the largest percent deviations, ca. 0.45%, have opposite sign. Anharmonicity in the C−H stretching region is discussed below.

Induction of Raman Intensity in T_{1g}, T_{2g}, and G_g Modes. Features observed in the INS spectrum at 632, ca. 845, 1007, 1282, and 1310 cm^{-1} have been assigned[8] as due to modes of T_{2g}, G_g, G_g, G_g, and T_{2g} symmetry, respectively (Table 1). These modes, and one T_{1g} mode calculated to be at 1305 cm^{-1} that was not identified in the INS spectrum, may exhibit Raman activity in the crystal symmetry point group. The G_g modes should be split into T and A components in the crystal field. Weak features are observed in the Raman spectra at 631 and 1005 cm^{-1} corresponding to the expected T_{2g} and G_g modes. The G_g mode expected at ca. 845 cm^{-1} is obscured by a strong H_g mode. The Raman spectrum from 1200 to 1350 cm^{-1} is shown on an expanded scale in Figure 4. On the basis of DFT calculations we expect modes of T_{2u}, G_g, T_{1g} T_{2g}, H_u, T_{1u}, G_u, and H_g symmetry in order of increasing frequency (Table 1). These modes are highly overlapped in the INS spectrum. The H_g Raman active mode is observed at 1326.9 cm^{-1}, and the IR active T_{1u} mode is observed at 1298.1 cm^{-1}. There should be crystal-induced intensity in the modes of G_g (T_g and A_g in T_h), T_{1g}, and T_{2g} symmetry. According to the DMol[3] calculations these should be at 1242 (1240.5, 1244), 1268.3, and 1274.7 cm^{-1}, respectively. The observed Raman features are at 1238.5, 1246, 1255.5, 1268.5 (shoulder), and 1275 cm^{-1}. If we assign the first and last two of these to the computed transitions, the degree of agreement is excellent with a root-mean-square deviation of only 1.4 cm^{-1}. The feature at 1255 remains assigned. A likely assignment is $2 \times T_{2g} = 2 \times 632.4 = 1265$ cm^{-1}.

Induction of IR Activity in Modes of Ungerade Symmetry. The ungerade modes of T_{2u}, G_u, and H_u symmetry are expected to become active in the IR spectrum in T_h. The H_u modes should be split into T_{1u} and E_u components, but only the T_{1u} component will have IR intensity. The observed and expected induced IR modes are shown in Table 1, where they are compared with calculated frequencies and assigned features of the INS spectrum. The features can all be seen in the IR trace of Figure 2. Figure 5 shows an expanded plot of the 1000−1200 cm^{-1} region

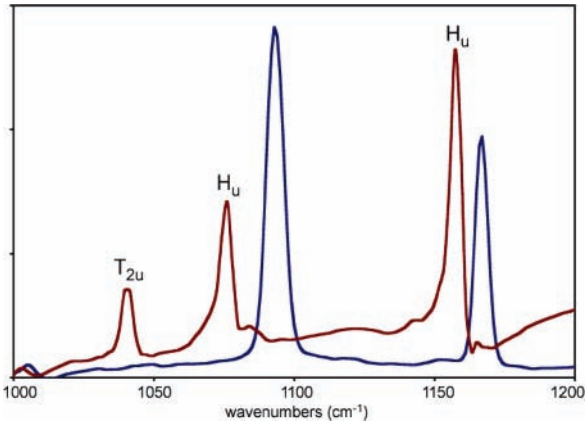

Figure 5. Raman (blue) and IR (red) spectra of dodecahedrane in the 1000−1200 cm^{-1} region. Three crystal-induced IR transitions are observed in this region. The two Raman transitions are symmetry allowed in I_h symmetry. Note the lack of any IR intensity in these transitions.

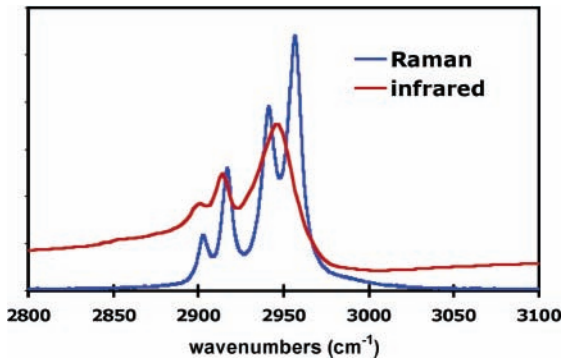

Figure 6. IR (red) and Raman (blue) spectra of dodecahedrane in the region from 2800 to 3100 cm^{-1} encompassing the fundamental region of the C−H stretching vibrations.

with the induced IR active modes compared with the H_g Raman active modes in this region. The lack of coincidence between the IR and Raman spectra is, of course, the signature of preservation of a center of inversion. The T_{2u} and two H_u (T_{1u}) transitions that are computed to be at 1055.8, 1095.5, and 1151.7 cm^{-1} are observed at 1040.6, 1076.3, and 1157.4 cm^{-1}. The degree of agreement is not as good as for the similar induced Ramam modes discussed above. Weak bands at 1004 and 1224 cm^{-1} are assigned as the combinations [477 (H_g) + 514 (H_u)] and [607 (G_g) + 632 (T_{2g})], respectively. Each of the combinations has a T_{1u} (T_u in T_h) component which will be in Fermi resonance with an adjacent T_{1u} (T_u) fundamental.

C−H Stretching Region. In the region above 2800 cm^{-1} there are six modes expected with T_{1u}, T_{2u}, G_u, A_g, G_g, and H_g symmetry in I_h. It is expected that there will be three features in the Raman spectrum: the A_g mode and the T and E components of the H_g mode. Weak activity is also expected in the G_g mode induced by the site symmetry. DFT calculations for the isolated molecule indicate that the state ordering of the gerade modes should be $A_g > H_g > G_g$. One of the features in the Raman spectrum in this region (Figure 6) must be due to field-induced intensity in one of the components of the G_g mode. Similarly, the IR spectrum in this region exhibits three features. Only one IR transition is expected for I_h symmetry. The other two features must be induced by the T_h field.

Comparison with a Periodic DFT Calculation

The effect of the packing interactions in the T_h site symmetry on the structure of dodecahedrane can be computed using a

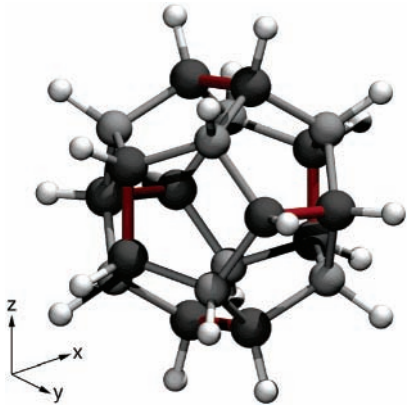

Figure 7. Structure of dodecahedrane in its crystal T_h site symmetry as determined from a DMol^3 calculation. The six bonds shown in red have a length of 1.55844 Å while the remaining 24 bonds have a length of 1.55742 Å. The six lengthened bonds are arranged in T_h symmetry in such a way that the 5-fold symmetry axis is lost but the inversion center is retained.

periodic DFT calculation. Such a calculation has been performed using the DMol^3 method. Some deformation of the I_h structure in the T_h symmetry environment is mandated by the lower symmetry of the site symmetry compared to the molecular symmetry. This deformation is the origin of the splitting of the Raman transitions of H_g symmetry. The issue here is the size of that deformation for such a rigid molecule and the degree to which it is reflected in the calculation and in the X-ray diffraction data. The structure obtained in the DMol^3 calculation has six C−C bonds with a length of 1.55844 Å arranged in a tetrahedral fashion (tangential to the body diagonals of a cube as shown in Figure 7) and 24 C−C bonds of 1.55742 Å. The two reported X-ray diffraction structures of dodecahedrane give bond lengths of 1.545(1) and 1.544(4) Å [1] and 1.541(2) and 1.535(5) Å,[6] respectively. The calculated difference in the bond lengths of 0.001 Å is thus in excellent agreement with the more recent and more precise determination.[1] It should be noted, however, that the error limits of the X-ray data preclude a precise determination of this deformation which is presumably the origin of the splitting of the H_g Raman active vibrations.

The average C−C bond length reported[1] for dodecahedrane, 1.544 Å, is considerably shorter than the computed value of 1.558 Å. A similar discrepancy was previously noted for the similar case of pagodane.[17] The origin of this discrepancy may be some minor static or dynamic disorder of dodecahdedrane in its crystal at low temperature. This has been discussed for this specific case and also for the hydrocarbon cubane by Dillen.[18,19] In the case of dodecahedrane,[19] Dillen shows that a 4° rotation of the $C_{20}H_{20}$ unit around a body diagonal results in an apparent shortening of the C−C bond by 0.011 Å. On the basis of an empirical force field model Dillen argues that such disorder will occur in this crystal at room temperature. If we apply this correction to the more recent X-ray data, the average bond length becomes $1.544 + 0.011 = 1.555 \pm 0.003$ Å. The computed value differs by one standard deviation from the corrected experimental result. The correction depends on the estimate of the degree of disorder and thus might be larger.

This DMol^3 calculation may be used to compute the splitting of the Raman active H_g modes. The calculated and observed frequencies and their differences are shown in Table 2. The difference in the two calculated components for each H_g mode, i.e., the calculated splitting, is always larger than the observed splitting. For the three lower frequency modes, this ratio of calculated to observed values is ca. 1.5−2. These are predominantly carbon skeletal modes. The higher modes are primarily C−H wagging vibrations and exhibit larger discrepancy.

The INS spectrum of dodecahedrane has previously been interpreted in terms of a DFT calculation for the isolated molecule using Gaussian98. Here the results of the periodic DFT calculation describing the crystal are compared to the experiment. To make this comparison more detailed, we include the overtone, combination, and phonon-wing excitations. These transitions are allowed in neutron scattering in the harmonic approximation with intensity that increases relatively with increasing momentum transfer Q.[20] The inclusion of multiquantum transitions is done using the aCLIMAX program.[21] The results are shown in Figures 8−10. It is observed that the full intensity profile is in excellent agreement with experiment from 400 to 1000 cm^{-1} with only minor disagreement at higher energy. The first-order phonon wings contribute by far the most significant multiquantum contribution to the spectrum in this region. Near 1300 cm^{-1} the phonon-wing contribution is roughly as large as that of the fundamental transition.

The INS spectrum of dodecahedrane has previously been interpreted in terms of a DFT calculation for the isolated molecule using Gaussian98.[8] Here the results of the periodic DFT calculation describing the crystal are compared to the experiment. This calculation is performed with the results of the $Z = 4$ $Fm\bar{3}$ cubic group. Since this is a "supercell" relative to the $Z = 1$ primitive unit cell, the motions of one molecule relative to another are included in the calculation. This is equivalent to inclusion of one state at the zone center and one at the zone boundary. However, the separation of the frequencies for these two states is very small in comparison to the resolution of the INS spectrometer. This is as expected since localized internal modes of motion for molecules show very little dispersion. In this comparison, we include the overtone, combination, and phonon-wing excitations in addition to the fundamental transitions. These transitions are allowed in neutron scattering in the harmonic approximation with intensity that increases relative to increasing momentum transfer Q.[20] The intensity for a transition to state i is proportional to $\sum_j b_j \exp(-Q^2U_j^2)(U_{ij}Q)^{2n}$, where j labels the atoms of cross section b_j, n is the overtone or combination order, U_{ij} is the amplitude of motion of atom j in mode i, and U_j^2 is the sum over all normal modes of the squared amplitude of atom j.[21] Since both Q and the density of such overtones increase with energy transfer, these transitions have increasing importance at higher energy transfer. The inclusion of multiquantum transitions is done using the aCLIMAX program.[21] The results are shown in Figures 8 and 9. It is observed that the full intensity profile is in excellent agreement with experiment from 400 to 1000 cm^{-1} with only minor disagreement at higher energy. The first-order phonon wings contribute by far the most significant multiquantum contribution to the spectrum in this region. Near 1300 cm^{-1} the phonon-wing contribution is roughly as large as that of the fundamental transition.

The 1600−4000 cm^{-1} region shown in Figure 9 includes the C−H stretch region. All of the intensity in the 1600−2800 cm^{-1} region is accounted for by binary overtones and the ternary transitions (Q^6 dependence) due to phonon wings on the binary transitions. The region above 3100 cm^{-1} is dominated by 0−3 transitions and their added phonons. The feature at 3000 cm^{-1} is associated with the fundamental of the C−H stretch band of transitions. This central part of the spectrum is shown in expanded form in Figure 10, where it is compared with the Raman spectrum. Figures 9 and 10 show this feature as calculated and also with the C−H fundamental transition

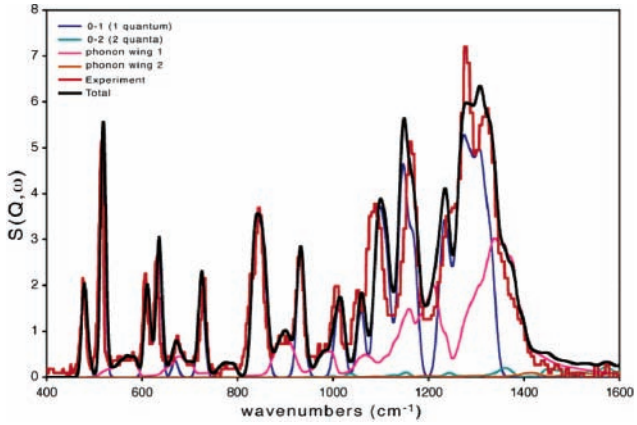

Figure 8. Inelastic neutron scattering spectrum of dodecahedrane from 400 to 1600 cm^{-1}. The red trace is the experimental spectrum. The black trace is the spectrum computed on the basis of a DMol[3] computation for the $Z = 1$ primitive cell using the room-temperature lattice parameters with inclusion of combinations and overtones using the program aCLIMAX. The intensity due to the fundamental (0→1) transitions only is shown in blue. The intensity of the 0→2 transitions is shown in light blue and is very weak in this region. The intensity of the phonon-wing transitions as sidebands on the 0→1 transitions is shown in light red. The experimental phonon wing was used for the calculation of the phonon wings. See Figure 11.

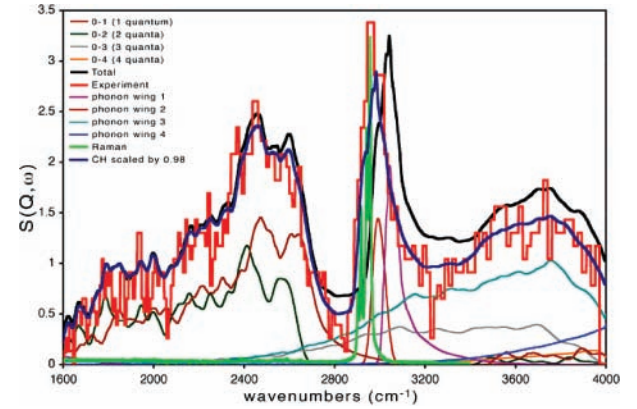

Figure 9. INS (red) and Raman (green) spectra of dodecahedrane in the region from 1600 to 4000 cm^{-1}. The DMol[3]/aCLIMAX spectrum is shown in black and also in blue where the C−H stretch fundamental has been adjusted downward in frequency by a factor of 0.98. The unadjusted 0→1 fundamental contribution near 2900 cm^{-1} is shown in rust. The phonon-wing sideband to this transition is shown in purple. The region between 1600 and 2800 cm^{-1} is dominated by the two-quanta combinations and overtones (green) and the phonon sidebands on these transitions (dark plum). The region above 3100 cm^{-1} is dominated by three-quanta combinations and overtones in gray and, especially, the phonon wings on these transitions shown in dark cyan.

frequencies scaled uniformly by a factor of 0.98 to account for the well-known anharmonicity of this degree of freedom. The intensity of the INS spectrum due to the phonon wing on the 0−1 transition is stronger than that of the fundamental transition due to the high value of Q in this region of energy transfer.

This DMol[3] calculation can serve as a guide to the assignment of the Raman and IR spectra in the C−H stretching region shown in Figure 6. Table 3 shows the computed frequencies and their symmetries in this region. The symmetries are given for the T_h site symmetry of the crystal and also as the approximate I_h symmetry in order to show the source of the first-order Raman (A_g and H_g) and IR (T_{1u}) intensities. The highest frequency and strongest feature in the Raman spectrum at 2957.1 cm^{-1} is identified with the A_g Raman active transition calculated at 3030.5 cm^{-1}. The ratio of these frequencies is

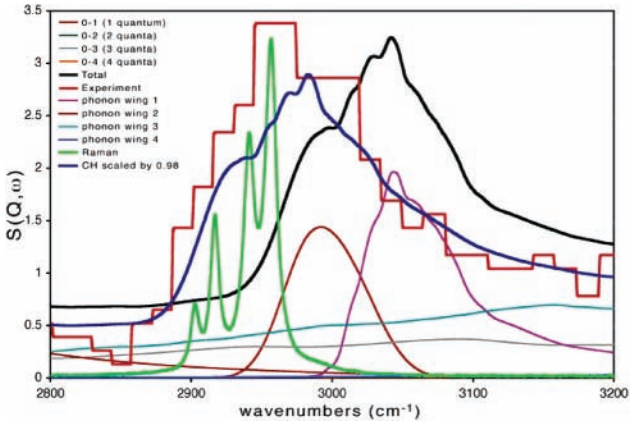

Figure 10. INS and Raman spectra of dodecahedrane in the C−H stretch region on an expanded scale to show the fundamental transition in more detail.

TABLE 3: Calculated and Observed Vibrations in the C−H Stretch Region

			observed		
T_h	I_h	calcd	Raman	IR	ratio[a]
T_u	T_{2u}	2970.5		2900.5	0.976
T_g	G_g	2972.7	(2903.8)		(0.977)
A_g	G_g	2981.6	2903.8		0.974
T_u	G_u	2987.0		2912.5	0.975
E_g	H_g	2992.1	2917.5		0.975
A_u	G_u	3003.0			
T_g	H_g	3003.6	2941.7		0.979
T_u	T_{1u}	3013.2		2947.2	0.978
A_g	A_g	3030.5	2957.1		0.976

[a] The ratio indicates the anharmonicity.

0.976, as shown in the last column. This is consistent with the anharmonicity of the C−H deformation motion. The next lower frequency motion is a T_u mode that has T_{1u} parentage and thus IR activity in I_h and is assigned to the highest energy, strongest IR mode. The next two gerade symmetry modes are a pair derived from the Raman active H_g mode of I_h symmetry. These are assigned to the next two Raman transitions at 2941.7 and 2917.5 cm^{-1}. The calculated splitting of this H_g mode of 11.5 cm^{-1} is considerably smaller than the observed value of 24.2 cm^{-1}, the pattern opposite to that seen for the lower frequency H_g modes. A mode of A_u symmetry is intercalated between these two components with H_g parentage. This inactive mode is the upper component of a G_u mode. The lower component of T_u symmetry is expected to have IR activity and is assigned to the next IR feature at 2912.5 cm^{-1}.

There are then three remaining computed vibrations to which one Raman and one IR transition must be assigned. In each case the intensity for these vibrations must be induced in the recipient mode by the T_h crystal deformation. The IR mode must be assigned to the only remaining ungerade mode, that of T_u symmetry calculated at 2970.5 cm^{-1} and observed at 2900.5 cm^{-1}. The induced Raman mode observed at 2903.8 cm^{-1} may be assigned equally to either the A_g or the T_g modes.

The low-frequency or phonon region of the dodecahedrane spectrum is shown in Figure 11, where it is compared with the result of the $Fm\bar{3}$ $Z = 4$ calculation. This calculation includes the translational motions at $k = 0$ and $k = \pi/a$ as well as the librons at these two limits. The $Z = 1$ primitive cell calculation has a single degenerate libron at 18.8 cm^{-1}. The $Z = 4$ calculation places the triply degenerate torsional phonons at 12.4, 41.4, and 44.7 cm^{-1}. Thermal population of these modes may be the origin of the C−C bond shortening effect noted above.

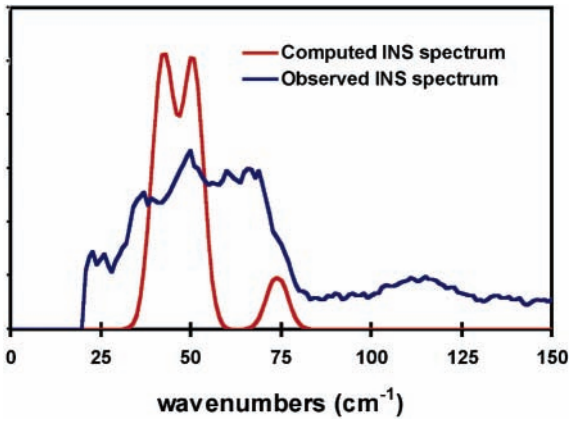

Figure 11. Inelastic neutron scattering spectrum of dodecahdedrane in the 0−150 cm^{-1} region showing the lattice vibrations (blue) compared to the computed spectrum from the $Fm\bar{3}$ $Z = 4$ cell (red). The experimental region from 0 to 80 cm^{-1} was used to simulate the phonon wings that contribute sidebands on the internal vibrations.

The triply degenerate high k translational phonons are computed to be at 50.4, 51.3, 52.3, and 74.4 cm^{-1}. These are the top of the dispersed phonons that extend to zero frequency at $k = 0$. The translational modes thus extend from lower to higher frequency than the torsional modes. The intensity above 90 cm^{-1} is due to phonon overtones. A more complete modeling of this phonon spectrum is of interest with respect to the hypothesized crystal disorder.

Discussion

The Raman and IR spectra of dodecahedrane in the C−H stretch and lower fundamental regions, as well as the extra features in the IR spectrum, clearly indicate that the site and thus molecular symmetry is not I_h as, of course, it cannot be. The vibrational spectra are sensitive to lattice-induced deformations that are at or near the limit of resolution of the existing diffraction data. The comparison of the computed and observed INS spectra in the high-frequency region (Figures 9 and 10) shows that decomposition of the overtone and combination contributions that dominate this region is possible without adjustable parameters other than a uniform anharmonic scaling of the C−H stretch fundamentals. This excellent agreement between the computed and observed INS spectral intensity distribution derives, in part, from the fact that dodecahdedrane is an isotropic system so that assumptions of this symmetry inherent in the overtone and combination intensity simulations are valid. The excellent overall agreement between the computed and observed vibrational spectra demonstrates that the DMol^3 method applied to the existing crystal model provides an adequate description of the molecular dynamics including the splitting of the degenerate modes. It should be noted that this degree of agreement derives directly from the unscaled (except for the anharmonic C−H stretch) computed frequencies and an overall intensity factor. There are, thus, only two adjustable parameters in the overall fit to the INS spectra, one of which can be obtained by comparison of the computed C−H region frequencies and the high-resolution Raman data.

It seems likely that at room temperature there is some degree of dynamic disorder in these crystals that contributes to the Raman line widths, resulting in the smaller than expected vibrational splittings of the H_g Raman active modes and producing the shortening of the apparent bond lengths deduced from the crystallographic analysis. A previous estimate of the magnitude of this effect indicates that the computed C−C bond length is very close to the actual value in the crystal. If this disorder is static rather than dynamic, it may be necessary to interpret the diffraction and spectral data accordingly.

The general message of this study is that even simple alkanes, despite the weak nature of their intermolecular interactions, are deformed in their crystalline lattice. While this distortion may be at the limit of diffraction data, it is easily seen in optical vibrational spectroscopy for high-symmetry systems.

Acknowledgment. The Rutherford Appleton Laboratory is thanked for neutron beam access at the ISIS Facility where the TOSCA spectrometer was used. This work was supported by US National Science Foundation Grant CHE 0240104 and by the US Department of Energy Grant DE-FG02-01ER14245. The National Center for Supercomputing Applications, University of Illinois at Urbana−Champaign, is thanked for access to the SGI Origin Array for the DMol^3 calculations. Graphics were rendered with VMD.[22] We thank Dr. Nina Verdal for a careful reading of the manuscript that resulted in several significant changes.

References and Notes

(1) Bertau, M.; Wahl, F.; Weiler, A.; Scheumann, K.; Wörth, J.; Keller, M.; Prinzbach, H. *Tetrahedron* **1997**, *53*, 10029−10040.

(2) Bertau, M.; Leonhardt, J.; Weiler, A.; Weber, K.; Prinzbach, H. *Chem.−Eur. J.* **1996**, *2*, 570−579.

(3) Pinkos, R.; Weiler, A.; Voss, T.; Weber, K.; Wahl, F.; Melder, J. P.; Fritz, H.; Hunkler, D.; Prinzbach, H. *Liebigs Ann./Recl.* **1997**, 2069−2088.

(4) Paquette, L. A.; Ternansky, R. J.; Balogh, D. W.; Kentgen, G. *J. Am. Chem. Soc.* **1983**, *105*, 5446−5450.

(5) Ternansky, R. J.; Balogh, D. W.; Paquette, L. A. *J. Am. Chem. Soc.* **1982**, *104*, 4503−4504.

(6) Gallucci, J. C.; Doecke, C. W.; Paquette, L. A. *J. Am. Chem. Soc.* **1986**, *108*, 1343−1344.

(7) It is, however, the $Z = 1$ primitive unit cell that determines the presence of any factor group splitting. Fateley, W. G.; Dollish, F. R., McDivitt, N. T.; Bentley, F. F. *Infrared and Raman Selection Rules for Molecular and Lattice Vibrations: The Correlation Method*; Wiley-Interscience: New York, 1972.

(8) Hudson, B. S.; Braden, D. A.; Parker, S. F.; Prinzbach, H. *Angew. Chem., Int. Ed.* **2000**, *39*, 514−516 [*Angew. Chem.* **2000**, *112*, 524−526].

(9) Parker, S. F.; Carlile, C. J.; Pike, T.; Tomkinson, J.; Newport, R. J.; Andreani, Ricci, F. P.; Sachetti, F.; Zoppi, M. *Physica B* **1998**, *154*, 241−243.

(10) Colognesi, D.; Celli, M.; Cilloco, F.; Newport, R. J.; Parker, S. F.; Rossi-Albertini, V.; Sacchetti, F.; Tomkinson, J.; Zoppi, M. *Appl. Phys. A: Mater. Sci. Process.* **2002**, *74* (Suppl., Pt. 1), S64−S66.

(11) Parker, S. F. *J. Neutron Res.* **2002**, *10*, 173−177.

(12) Delley, B. *J. Chem. Phys.* **1990**, *92*, 508−517.

(13) Delley, B. *J. Chem. Phys.* **1991**, *94*, 7245−7250.

(14) Delley, B. *Comput. Mater. Sci.* **2000**, *17*, 122−126.

(15) Delley, B. *J. Chem. Phys.* **2000**, *113*, 7756−7760.

(16) Burke, K.; Perdew, J. P.; Wang, Y. In *Electronic Density Functional Theory and New Directions*, Dobson, J. F., Vignale, G., Das, M. P., Eds.; Plenum: New York, 1998.

(17) Allis, D. G.; Prinzbach, H.; Hudson, B. S. *Chem. Phys. Lett.* **2004**, *386*, 356−363.

(18) Dillen, J. L. M. *S. Afr. J. Chem.* **1991**, *44*, 62−63.

(19) Dillen, J. *J. Phys. Chem. A* **2000**, *104*, 7734−7737.

(20) Hudson, B. S. *J. Phys. Chem. A* **2001**, *105*, 3949−3960.

(21) Ramirez-Cuesta, A. J. *Comput. Phys. Commun.* **2004**, *157*, 226. (aCLIMAX is available at http://www.isis.rl.ac.uk/molecularSpectroscopy/.) The amplitude of atomic motion U that appears in the Debye−Waller factor $\exp(-Q^2U^2)$ includes both internal and external motions of the molecule. aCLIMAX treats the external motion in terms of the Sachs−Teller method, which is a gas approximation. The experimental phonon spectrum (Figure 11, 0−80 cm^{-1}) is used as input to aCLIMAX for the simulation of the phonon sidebands.

(22) Humphrey, W.; Dalke, A.; Schulten, K. *J. Mol. Graphics* **1996**, *14*, 33−38.